Solid State Ionics 262 (2014) 292–297

Contents lists available at ScienceDirect

Solid State Ionics

journal homepage: www.elsevier.com/locate/ssi

High Performance Mixed-Potential Type NO_x Sensor Based On Stabilized Zirconia and Oxide Electrode

Geyu Lu *, Quan Diao, Chenguo Yin, Shiqi Yang, Yingzhou Guan, Xiaoyang Cheng, Xishuang Liang

State Key Laboratory on Integrated Optoelectronics, College of Electronic Science and Engineering, Jilin University, 2699 Qianjin Street, Changchun 130012, China

ARTICLE INFO

Article history:
Received 17 May 2013
Received in revised form 16 January 2014
Accepted 20 January 2014
Available online 23 February 2014

Keywords:
Mixed-potential
YSZ gas sensors
Microstructure
TPB

ABSTRACT

The mixed-potential NO_x sensor based on yttria-stabilized zirconia (YSZ) and oxide electrode is considered as a potential device used for the on-board diagnostics. Over the past decades, many researchers have paid their attentions on such YSZ based potentiometric NO_x sensors and gotten a lot of achievement in developing new type electrode materials. Recently, in order to enhance the sensing performance of the mixed potential type NO_x sensor, we have been focusing on modifying the triple-phase-boundary (TPB) by various techniques, including chemical corroding, the double-tape casting, the pore-forming and laser fabrication method. We also designed and prepared the microstructure of the oxide electrodes by controlling the sintering process for increasing the sensitivity of the NO_x sensor. This paper reviews our works with regard to the above-mentioned two aspects.

1. Introduction

With speedy increase of the vehicles in city, the car exhaust results in severe urban atmosphere pollution. More and more attentions have been focused on the detection of nitrogen oxides (NO_x) which give rise to some environmental disasters such as acid rain and photochemical smog. To monitor and detect the NO_x from car exhaust, the high performance NO_x sensor has been urgently desired. Because the NO_x sensor used for monitoring the car exhaust must work under very harsh condition (high temperature, high humidity and many coexisting gases), the sensor materials used for the NO_x sensor should have excellent chemical and thermal stability. The stabilized zirconia and the metal oxides show the advantage in the stability under the severe atmosphere, so the mixed potential type NO_x sensors based on them have been widely investigated [1–13].

Since the oxide electrodes play an important recognition role for NO_x molecules, most of the researchers have paid more attentions for developing new oxide electrodes. Some single (WO_3 [14–21], NiO [22–25] and Cr_2O_3 [26–28]) and complex (spinel and perovskite type) oxides have been applied as the sensing electrodes of the YSZ-based NO_x sensors. For the study of the oxide sensing electrode, both composition and microstructure of the electrode materials have attracted special attentions, because the composition and microstructure decide the catalytic (electrochemical and chemical) activity and diffusion speed of the gases, respectively. On the other hand, the triple-phase-boundary (TPB) where the electrochemical reactions take place is very important for enhancing the sensing performance. The TPB with a large area can give more electrochemical activity sites, so its constructing strategy has been investigated by some researchers. J. Park et al. raised the area of TPB by mixing NiO with YSZ [12], but such method also covered some activity sites, resulting in the decrease of the electrochemical reaction rate. We have suggested another strategy: forming a rough surface of YSZ plate which does not only give a larger contacting interface between the YSZ plate and the sensing electrode, but also keep a higher activity of the electrode materials. Some rough surfaces of YSZ plates have been fabricated with some special surface treatment techniques by our group, such as HF corroding, the double-tape casting, the pore-forming and laser fabrication methods. In this paper, we will review the development of new sensing electrode materials and the construction of the TPB with large area.

2. Development of the novel sensing electrode materials

The composition of the sensing electrode materials plays an important role on the sensing property of the mixed potential NO_x sensor based on YSZ. The oxide sensing electrodes were testified to have better sensing performance (sensitivity and selectivity to NO_x) than the noble metals [20–27]. Some typical simple and complex oxides oxide electrode materials are summarized in the Table 1. For the simple oxide electrodes, NiO, Cr_2O_3, WO_3, ZnO, In_2O_3, CuO and V_2O_5 have been widely investigated by some groups. Among them, NiO shows very excellent sensing property at elevated temperature. The sensitivity of the NO_2 sensor based on NiO is about 40 mV/decade in the early study. The sensor output (ΔEMF) can be improved by optimizing the sintering temperature of NiO, because an appropriate sintering temperature can form the best balance among the electrochemical and chemical activities as well as porosity for NiO [29]. In addition, the resistance of NiO to water vapor [30] has been studied. The sensor using NiO sensing electrode shows good output even in wet atmospheres with different O_2

* Corresponding author. Tel./fax:86431 85167808.
E-mail address: lugy@jlu.edu.cn (G. Lu).

0167-2738/$ – see front matter © 2014 Published by Elsevier B.V.
http://dx.doi.org/10.1016/j.ssi.2014.01.037

Table 1
Typical example of the SE materials for mixed-potential type NOx sensors.

Sensing electrode materials	Operating temperature (°C)	Reference
NiO	900	[22–25]
ZnO	600 ~ 700	[34]
CuO	700	[12]
WO_3	500 ~ 700	[14–21]
Cr_2O_3	500	[27]
In_2O_3	550	[46]
V_2O_5	440	[33]
Rh-loaded NiO	800	[23]
Tin-doped indium (ITO)	613	[13]
$NiCr_2O_4$	550	[35]
$MnCr_2O_4$	650	[37]
$ZnCr_2O_4$	700	[48]
$ZnFe_2O_4$	650	[49]
$CdCr_2O_4$	500 ~ 600	[36]
CuO + $CuCr_2O_4$	518-659	[47]
$LaFeO_3$	450	[38]
$La_{0.8}Sr_{0.2}FeO_3$	450 ~ 700	[39]
$La_{0.6}Sr_{0.4}Fe_{0.8}Co_{0.2}O_3$	500	[40]
$La_{0.85}Sr_{0.15}CrO_3$	600	[41]
NiO + YSZ	700	[12]

concentration [31]. Doping of noble metals or oxides in NiO is also a strategy to increase the sensing performance. For example, the Rh-loaded NiO sensing electrode shows higher response to NO_2 than pure NiO, because high distribution Rh nanoparticle has higher electrochemical catalytic activity to the reaction related to NO_x [23]. Besides NiO, WO_3 and Cr_2O_3 also exhibit good sensing performance to NO_2. WO_3 fabricated with difference methods has unique microstructure which leads to different response [32]. However, WO_3 has been testified to be unstable at elevated temperature, so its thermal and chemical stabilities need to be improved by adding the other oxides. Other simple metal oxides, such as V_2O_5 [33], ZnO [31] and CuO [12], have also been reported as the sensing electrode materials.

In order to further increase the sensitivity of the mixed potential type NO_x sensor, some complex oxides oxides were prepared and utilized as the sensing electrodes. Lu and Mirua et al. firstly applied spinel type oxides for detecting NO_x. [35,36]. Specially, $NiCr_2O_4$ and $CdCr_2O_4$ displayed high sensitivity and excellent selectivity to NO_2 and NO at elevated temperature (Fig. 1). Recently, Diao et al. developed a new type spinel oxide electrode $MnCr_2O_4$ as the sensing electrode of the mixed potential type NO_x sensor [37]. The EMF of the sensor based on the $MnCr_2O_4$ is strongly dependent on its sintering temperature. As shown in Fig. 2, the optimal sintering temperature for the $MnCr_2O_4$ is 1000 °C. Generally, with the increasing of the sintering temperature, the electrochemically catalytic activity decreases, but the porosity increases. The former trend to reduce the sensitivity and the latter enhances the diffusion of the target gas into the sensing electrode layer and raises the sensor output. At 1000 °C, the best balance between the

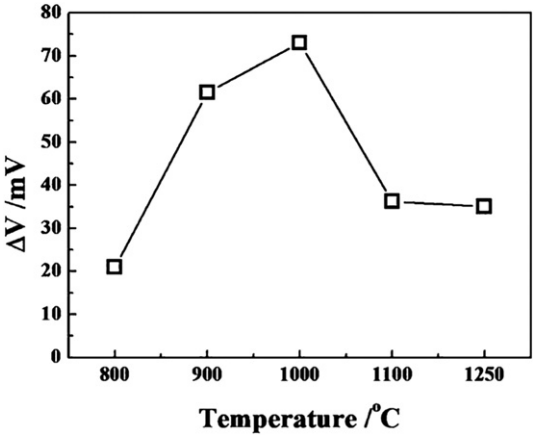

Fig. 2. Response to 100 ppm NO_2 of sensors based on $MnCr_2O_4$ calcined at different temperatures. Source: reprinted from reference [37] with permission from Elsevier.

above factors was obtained, and the largest output was realized. The measurement of the polarized curves for the sensors using the $MnCr_2O_4$ obtained at different the sintering temperature indicates that the $MnCr_2O_4$ sample sintering at 1000 °C gives the largest reduction current related NO_2, at the same time, effectively suppresses the electrochemical oxidation reaction related to oxygen. The perovskite complex oxides oxide was also examined as the sensing electrode. Due to its high chemically catalytic activity, the target gas was largely consumed when it passed through the sensing electrode layer, inducing the sharp decreasing of the NO_x concentration. Therefore, at high temperature, the sensor based on the perovskite complex oxides oxide displayed a small output. However, for $LaFeO_3$ [38], when the other element (such as Sr, Co and Ni) replaced the A or B site partly or completely, an improving response to NO_x was obtained [39–41].

The microstructure of the electrode materials, such as the particle and pore sizes [29], is another key factor determining the sensitivity of the mixed potential type NO_x sensor, because it can influence the adsorption and desorption of the target gases on the sensing electrode materials as well as their diffusion in the sensing electrode layer. Before arriving at the three-phase-boundary, the target gas must passes through the layer of the sensing electrode and is consumed partly due to the chemical reaction in this process. Therefore, the porosity of the sensing electrode is supposed to be of great benefit to enhance the sensing property. Generally, two strategies were applied for improving the porosity of the sensing electrode: enlarging particle size by increasing the sintering temperature and controlling pore size and number by using special hard template. Lu et al. prepared the W/Cr binary oxides in which W was utilized as hard template, because it can sublimate after 800 °C and form stable porous structure even at very high temperature [42]. The porosity and composition of W/Cr complex oxides oxide

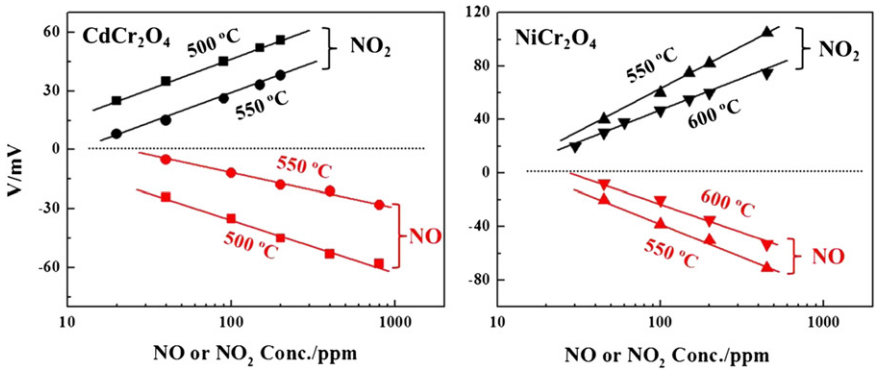

Fig. 1. Dependence of V on the logarithm of NO or NO_2 concentration for the mixed-potential-type device using the $CdCr_2O_4$ or $NiCr_2O_4$ SE. Source: reprinted from reference [35,36] with permission from Elsevier.

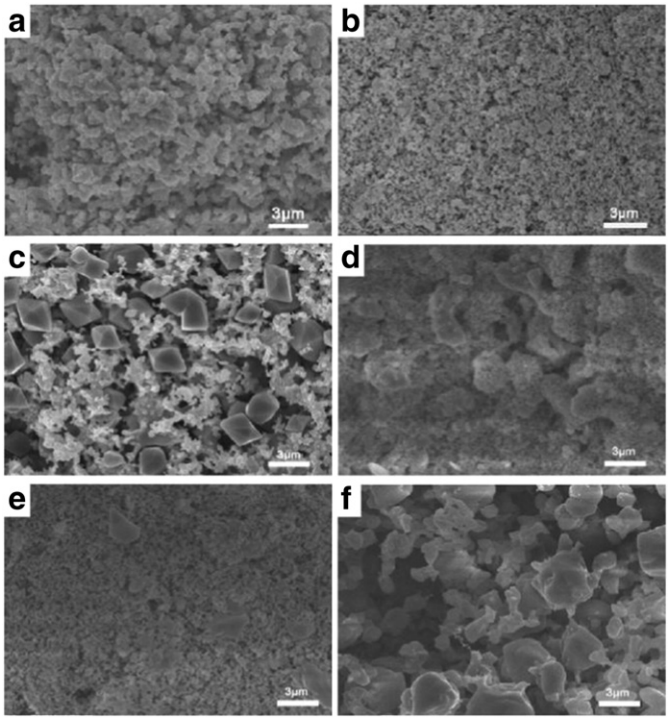

Fig. 3. (i) SEM images of electrode surfaces using W/Cr binary oxides as sensing materials with different ratios: (a) 1:6, (b) 1:2 and (c) 3:2 sintered at 1000 °C; (ii) electrode surfaces using W/Cr binary oxides with the ratio of 3:2 sintered at different temperatures: (d) 800 °C, (e) 900 °C and (f) 1100 °C. Source: reprinted from reference [42] with permission from Elsevier.

was strongly dependent on the molar ratio of W/Cr as well as sintering temperature [43]. As shown in Fig. 3, when the mole ratio of W/Cr was 3:2, the W/Cr complex oxides showed excellent porosity and forms new phase (Cr_2WO_6) surrounded by the small particle of WO_3. The sensor output was also related to the mole ratio of W/Cr and the sintering temperature (Fig. 4). The 3:2 W/Cr complex oxides oxides obtained at 1000 °C exhibited the largest sensor output. The above results indicate the importance of the porosity of the sensing electrode for the mixed potential type NO_x sensor.

3. Construction of the TPB

As expressed above, the three phase boundary is the field in which the electrochemical reactions related to the target gases take place. Therefore, its state is very important for the mixed potential type NO_x sensor. Some efforts have been carried out to prepare the high quality TPB. For example, Park et al. increased the contacting area of the sensing electrode and YSZ by adding YSZ powder to the NiO electrode material. We proposed a novel method for fabricating high performance TPB by covering the sensing electrode material on the porous YSZ surface, because the porous surface can supply larger surface area than planar one (Fig. 5). Three kinds of techniques, including the HF corroding [44], double-type casting [45] and laser fabricating methods, were used for fabricating the porous surface of YSZ substrate. The larger TPB can supply more active sites for the electrochemical reactions. Therefore, the sensing characteristics can be observably improved.

In our initial work, the YSZ plates were treated with different concentration HF: 0% HF (uncorroded), 10% HF, 20% HF and 40% HF. AFM measurement results indicated that the surface roughness of the corroded YSZ plate raised with the increasing of HF concentration as shown in Fig. 6. As forecasted, the sensor output became larger with the increasing of the surface roughness of the treated YSZ (Fig. 7), because the rougher YSZ surface can form larger contacting area and supply more activity sites for the related electrochemical reactions. From the response and recovery transients to different concentrations of NO_2 for the sensors based on the corroded YSZ plates, we found that the response speed was very fast for the all sensors using various roughness YSZ plates, but the recovery time became slower when the roughness was increased. Such sensing behavior can be attributed to the excellent porosity of the TPB which can enhance the adsorption of the target gas on the reaction sites and decrease the desorption of the reaction products.

We also tried to fabricate the porous surface of the YSZ plate by combining double-tape casting technique with the hard template method. The porous YSZ substrate was prepared with the following two steps: firstly, a layer of green tape was formed by using YSZ slurry without the hard template with a tape-casting unit; then, the YSZ slurry with starch was casted on the first green tape. After sintered, the first layer became dense while the second layer formed many pores on its surface. The SEM images of YSZ plates prepared with the slurry containing 0 wt%, 5 wt%, 10 wt% and 15 wt% starch indicated that. The density of pores on the surface of the YSZ plate increased with the increasing of the starch concentration (Fig. 8). The cross section view of the double-layer device (Fig. 8 (e) and (f)) proved that the oxide electrode closely contacted with the porous YSZ plate, resulting in the increasing of the reaction sites. The response and recovery transients to various concentrations of NO_2 for the sensors using the porous YSZ plates prepared by adding different concentration of starch testified that the sensor using the YSZ plate prepared from the slurry containing 15 wt % starches gave the largest response to the same concentration of NO_2 (Fig. 9). Such an enhancing sensing performance can be attributed to the increasing of the activity sites.

In our recent work, femtosecond laser direct writing technique has been used to prepare the regular pattern on the surface of the YSZ

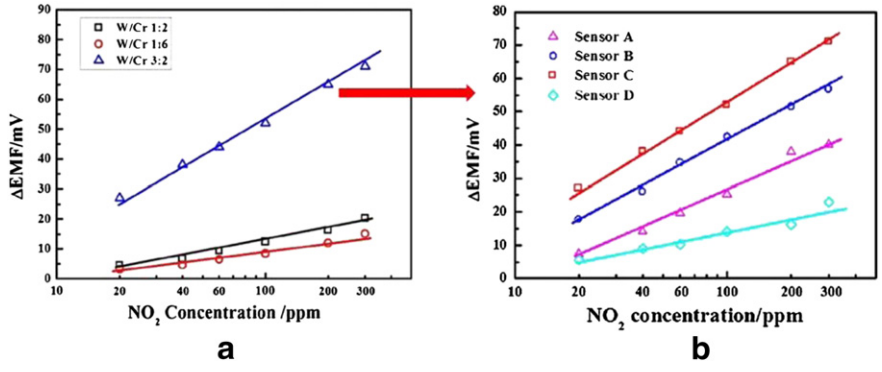

Fig. 4. (a) Dependence of the ΔEMF on the NO_2 concentrations in the range of 20–300 ppm for sensors using different W/Cr oxides sintered at 1000 °C as SE. Source: reprinted from reference [44] with permission from Elsevier. (b) Dependence of the ΔEMF on the NO_2 concentrations in the range of20-300 ppm for the sensors with ratio of 3:2 W/Cr oxides as SE sintered at different temperatures: (A) 800 °C; (B) 900 °C; (C) 1000 °C and (D) 1100 °C. Source: reprinted from reference [42] with permission from Elsevier.

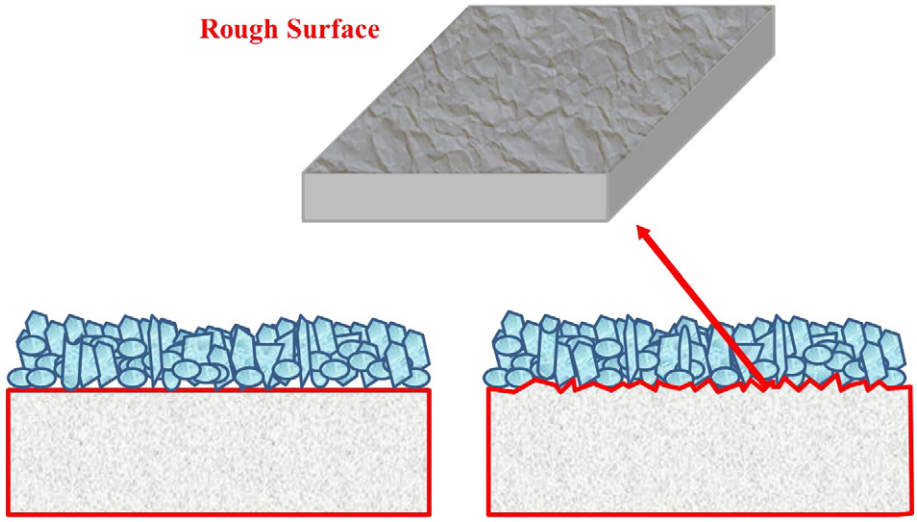

Fig. 5. Three-phase boundary of sensor: (a) plane and (b) three-dimensional.

substrate to build more excellent TPB. The laser pulse focused by convex lens can release a lot of heat at the focus which can induce the sublimation of YSZ surface where is radiated. Fig. 10 showed the SEM images of the as-treated YSZ substrate. The ravine on the as-treated YSZ surface gave larger contact area with the oxide electrode, obviously improving the sensing performance of the TPB based on the laser treated YSZ plate.

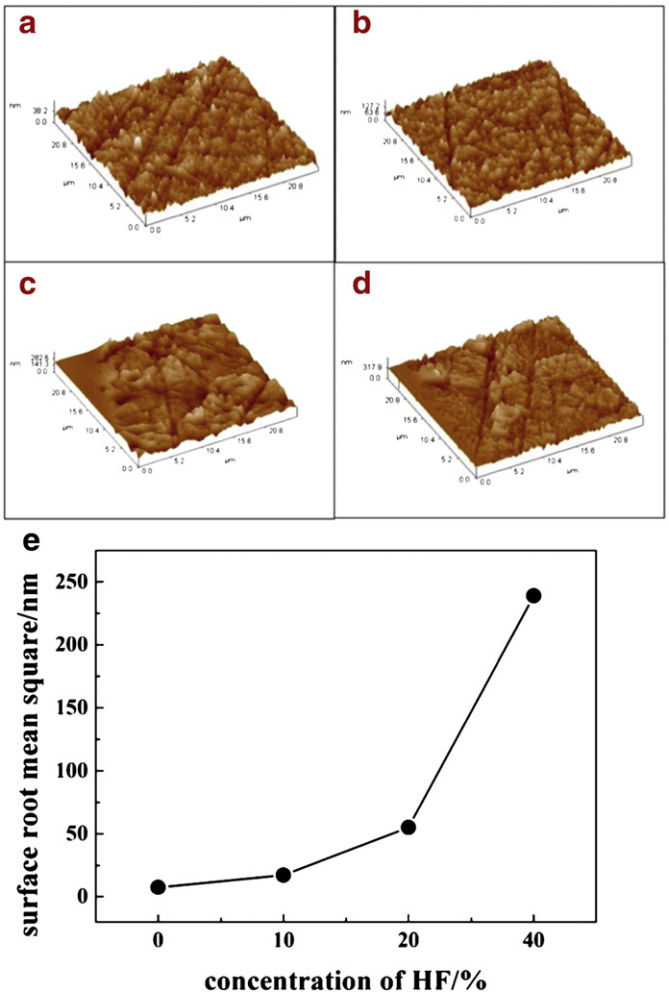

Fig. 6. AFM images of the surface of YSZ treated with different concentration HF: (a) uncorroded, (b) 10% HF, (c) 20% HF, (d) 40% HF and (e) surface root mean square of different surface root mean square. Source: reprinted from reference [44] with permission from Elsevier.

4. Sensing mechanism of the mixed potential NO_X sensor

The sensing behavior of this kind of potentiometric sensor can be explained by the mixed potential mechanism [30,46–49]. Lu and Miura et al. proposed the mixed potential mechanism for the high temperature gas sensors based on stabilized zirconia and oxide electrodes and examined the proposed mechanism by measuring the polarized curve. For simplifying the expression, we only considered the case of tubular type sensor: the sensing (oxide) electrode was exposed to the target gas, and the reference electrode is opened to air. Such a sensor can be described by the following electrochemical cells in target gas.

NO_2 (+ air), sensing electrode / YSZ / Pt, NO_2 (+ air)

$$\text{Cathodic}: NO_2 + 2e^- \rightarrow NO + O^{2-} \quad (1)$$

$$\text{Anodic}: 2O^{2-} \rightarrow O2 + 4e^- \quad (2)$$

$$E_M = E_0 + m\ln C_{NO2} - n\ln C_{O2} \quad (3)$$

Here, E0, m and n are the constants, and C_{NO2} and C_{O2} are the concentrations of NO_2 and O_2, respectively.

Under the target gas atmosphere, two electrochemical reactions (1) and (2) simultaneously take place at the sensing electrode. When the

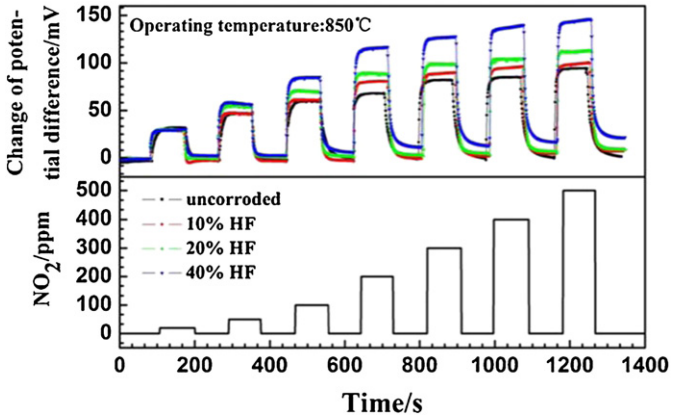

Fig. 7. The kinetic response of the sensor using YSZ treated with different concentration HF to 20–500 ppm NO_2. Source: reprinted from reference [44] with permission from Elsevier.

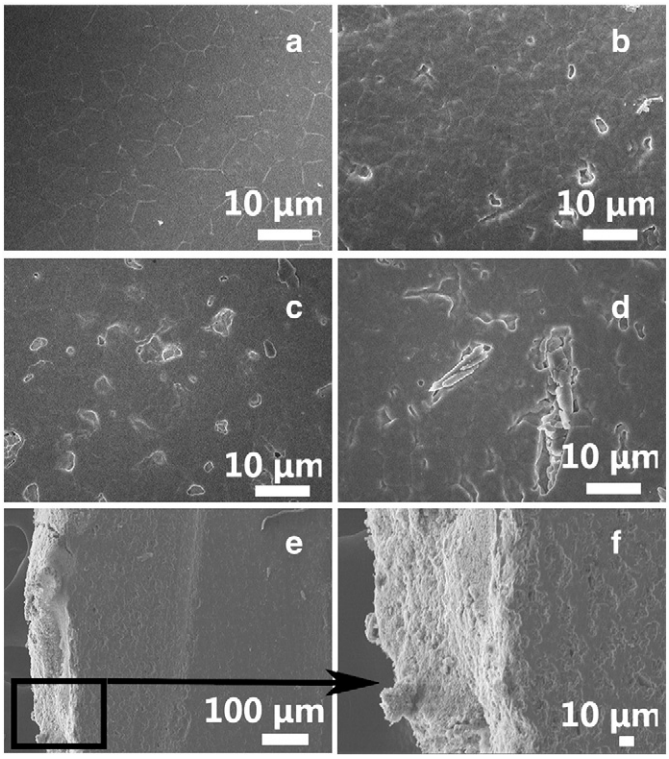

Fig. 8. SEM images of the YSZ-substrates fabricated by adding (a) 0 wt%, (b) 5 wt%,(c) 10 wt% and (d) 15 wt% starch sintering at 1500 °C and (e and f) the cross section view of the device. Source: reprinted from reference [45] with permission from Elsevier.

rates of reaction (1) and (2) are equal, a local cell forms and the potential in the sensing electrode is called the mixed potential. Its value is strongly dependent on the composition and microstructure of the sensing electrode materials, the state of the TPB as well as the concentrations of the target gas and oxygen. When the other factors are fixed, the magnitude of the mixed potential only depends on the concentration of the target gas, so the mixed potential is utilized as the sensing signal of this type of gas sensor. The correlation between the mixed potential and the concentration of the target gas was obtained by Lu et al. [36,37,42,44]. As expressed in Eq. (3), the sensing signal is linear with the logarithm of the concentration of the target gas, explaining the relationship between the EMF and the concentration obtained from the experimental

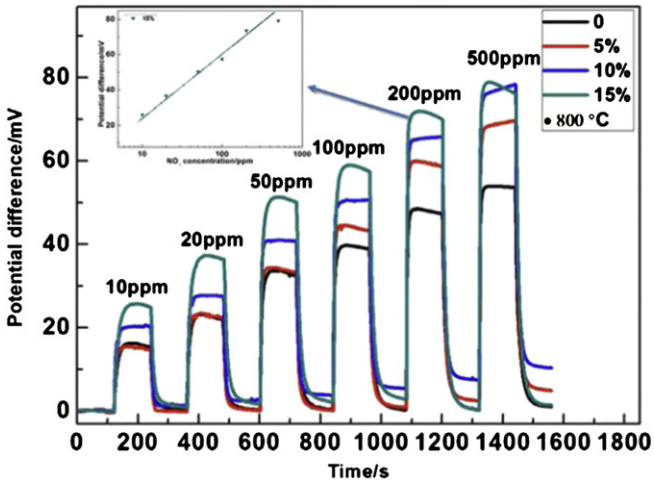

Fig. 9. Response transients of sensors using 0 wt%, 5 wt%, 10 wt% and 15 wt% starch to various NO_2concentrations in the range from 10 ppm to 500 ppm at 800 °C. Source: reprinted from reference [45] with permission from Elsevier.

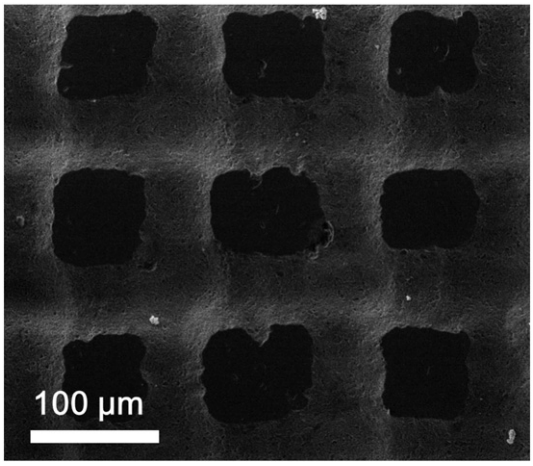

Fig. 10. SEM images of processed YSZ substrate.

data. The suggested sensing mechanism can be testified by the modified polarized curves related to the cathodic and anodic reactions, respectively. The intersection of the modified polarized curves corresponding to the cathodic and anodic reactions is the mixed potential determined by above two electrochemical reactions, having almost same value for every measuring concentrations. Such consistency has been examined for all oxide electrode materials developed by our group. As for the key factors decided the sensitivity of the mixed potential type NO_x sensor, some investigations have been carried out. However, the deep understanding for the sensing mechanism is still necessary.

5. Conclusion

The mixed-potential-type YSZ-based gas sensors have been investigated for a long period, and most of the researches were focused on the designing and developing of the new type electrode materials. However, the microstructure of electrode also plays an important role on the sensing performance. We paid special attention to the porosity of the oxide electrode materials. A serial of porous W/Cr binary oxides have been prepared by using WO3 as the high temperature hard template. We also prepared some porous spinel type complex oxides by controlling the sintering temperature. At the same time, we constructed the porous three phase boundary by using porous YSZ plate. Some fabricating strategies have been proposed by our group, such chemical corroding, double-tape casting as well as laser fabrication. Combing above fabricating techniques and the sintering methods, the sensing performance of the TPB was largely improved. The mixed potential sensing mechanism has further examined by the new type sensing electrode materials. For speeding up the practical application of this type of NO_X in the monitoring of the car exhausts, the long-term stability as well as the reliability in harsh using condition is needed to enhance.

Acknowledgements

This work was supported by the National Nature Science Foundation of China (Nos. 61074172, 61134010, 61104203), Program for Chang Jiang Scholars and Innovative Research Team in University (No. IRT1017) and “863” High Technology Project (2013AA030902).

Reference

[1] F. Ménil, V. Coillard, C. Lucat, Sensors Actuators B Chem. 67 (1–2) (2000) 1–23.
[2] S. Fischer, R. Pohle, B. Farber, R. Proch, J. Kaniuk, M. Fleischer, R. Moos, Sensors Actuators B Chem. 147 (2) (2010) 780–785.
[3] W. Göpel, Solid State Ionics 136–137 (1–2) (2000) 519–531.
[4] J.M. Rheaume, A.P. Pisano, Ionics 17 (2) (2011) 99–108.
[5] S. Fischer, R. Pohle, M. Fleischer, R. Moos, Procedia Chem. 1 (1) (2009) 585–588.
[6] L.Y. Woo, R.S. Glass, R.F. Novak, J.H. Visser, Sensors Actuators B Chem. 157 (1) (2011) 115–121.

[7] H.T. Giang, H.T. Duy, P.Q. Ngan, G.H. Thai, D.T.A. Thu, D.T. Thu, N.N. Toan, Sensors Actuators B Chem. 183 (2013) 550–555.
[8] M. Backhaus-Ricoult, K. Adib, K. Work, M. Badding, T. Ketcham, M. Amati, L. Gregoratti, Solid State Ionics 225 (2012) 716–726.
[9] F. Vanasscheiv, E. Wachsman, Solid State Ionics 179 (39) (2008) 2225–2233.
[10] J. Yoo, D. Oh, E. Wachsman, Solid State Ionics 179 (37) (2008) 2090–2100.
[11] J. Gao, J.-P. Viricelle, C. Pijolat, P. Breuil, P. Vernoux, A. Boreave, A. Giroir-Fendler, Sensors Actuators B Chem. 154 (2) (2011) 106–110.
[12] J. Park, B.Y. Yoon, C.O. Park, W.-J. Lee, C.B. Lee, Sensors Actuators B Chem. 135 (2) (2009) 516–523.
[13] X. Li, W. Xiong, G.M. Kale, Electrochem. Solid-State Lett. 8 (3) (2005) H27.
[14] N.F. Szabo, H. Du, S.A. Akbar, A. Soliman, P.K. Dutta, Sensors Actuators B Chem. 82 (2–3) (2002) 142–149.
[15] J.-C. Yang, P.K. Dutta, Sensors Actuators B Chem. 125 (1) (2007) 30–39.
[16] J.-C. Yang, P.K. Dutta, Sensors Actuators B Chem. 136 (2) (2009) 523–529.
[17] E. Di Bartolomeo, M.L. Grilli, J. Eur. Ceram. Soc. 25 (12) (2005) 2959–2964.
[18] J. Yoo, S. Chatterjee, E.D. Wachsman, Sensors Actuators B Chem. 122 (2) (2007) 644–652.
[19] C. López-Gándara, J.M. Fernández-Sanjuán, F.M. Ramos, A. Cirera, Solid State Ionics 184 (1) (2011) 83–87.
[20] S.P. Mondal, P.K. Dutta, G.W. Hunter, B.J. Ward, D. Laskowski, R.A. Dweik, Sensors Actuators B Chem. 158 (1) (2011) 292–298.
[21] E. Di Bartolomeo, N. Kaabbuathong, M.L. Grilli, E. Traversa, Solid State Ionics 171 (3) (2004) 173–181.
[22] P. Elumalai, N. Miura, Solid State Ionics 176 (31) (2005) 2517–2522.
[23] J. Wang, P. Elumalai, D. Terada, M. Hasei, N. Miura, Solid State Ionics 177 (2006) 2305–2311.
[24] V. Plashnitsa, T. Ueda, P. Elumalai, N. Miura, Sensors Actuators B Chem. 130 (1) (2008) 231–239.
[25] P. Elumalai, V.V. Plashnitsa, T. Ueda, M. Hasei, N. Miura, Ionics 12 (6) (2007) 331–337.
[26] T. Ono, M. Hasei, A. Kunimoto, N. Miura, Electrochemistry 71 (2003) 405–407.
[27] T. Ono, M. Hasei, A. Kunimoto, N. Miura, Solid State Ionics 175 (1) (2004) 503–506.
[28] L. Peter Martin, A. Quoc Pham, R.S. Glass, Sensors Actuators B Chem. 96 (1–2) (2003) 53–60.
[29] P. Elumalai, J. Wang, S. Zhuiykov, D. Terada, M. Hasei, N. Miura, J. Electrochem. Soc. 152 (7) (2005) H95–H101.
[30] N. Miura, J. Wang, M. Nakatou, Pe. Elumalai, S. Zhuiykov, M. Hasei, Sensors Actuators B 114 (2006) 903–909.
[31] D.L. West, F.C. Montgomery, T.R. Armstrong, Sensors Actuators B (111–112) (2005) 84–90.
[32] M.L. Grilli, L. Chevallier, M.L.D. Vona, S. Licoccia, E.D. Bartolomeo, Sensors Actuators B (111–112) (2005) 91–95.
[33] S. Käding, S. Jakobs, U. Guth, Ionics 9 (1–2) (2003) 151–154.
[34] S. Zhuiykov, T. Nakano, A. Kunimoto, N. Yamazoe, N. Miura, Electrochem. Commun. 3 (2) (2001) 97–101.
[35] N. Miura, G. Lu, N. Yamazoe, Sensors Actuators B Chem. 52 (1–2) (1998) 169–178.
[36] Q. Diao, C. Yin, Y. Guan, X. Liang, S. Wang, Y. Liu, Y. Hu, H. Chen, G. Lu, Sensors Actuators B Chem. 177 (2013) 397–403.
[37] N.N. Toan, S. Saukko, V. Lantto, Phys. B Condens. Matter 327 (2–4) (2003) 279–282.
[38] E. Di Bartolomeo, N. Kaabbuathong, M.L. Grilli, E. Traversa, Solid State Ionics 171 (3–4) (2004) 73–181.
[39] D.L. West, F.C. Montgomery, T.R. Armstrong, Ceram. Eng. Sci. Proc. 25 (3) (2004) 493–498.
[40] D.L. West, F.C. Montgomery, T.R. Armstrong, Sensors Actuators B 106 (2) (2005) 758–765.
[41] Q. Diao, C. Yin, Y. Liu, J. Li, X. Gong, X. Liang, S. Yang, H. Chen, G. Lu, Sensors Actuators B Chem. 180 (2013) 90–95.
[42] L.P. Martin, A.Q. Pham, R.S. Glass, Sensors Actuators B 96 (2003) 53–60.
[43] X. Liang, S. Yang, J. Li, H. Zhang, Q. Diao, W. Zhao, G. Lu, Sensors Actuators B Chem. 158 (1) (2011) 1–8.
[44] C. Yin, Y. Guan, Z. Zhu, X. Liang, B. Wang, Q. Diao, H. Zhang, J. Ma, F. Liu, Y. Sun, J. Zheng, G. Lu, Sensors Actuators B Chem. 183 (2013) 474–477.
[45] H. Jina, M. Breedon, N. Miura, Talanta 88 (2012) 318–323.
[46] W. Xiong, G.M. Kale, Sensors Actuators B Chem. 119 (2006) 409–414.
[47] N. Miura, M. Nakatou, S. Zhuiykov, Sensors Actuators B Chem. 4 (2002) 284–287.
[48] N. Miura, S. Zhuiykov, T. Ono, M. Hasei, N. Yamazoe, Sensors Actuators B Chem. 83 (2002) 222–229.
[49] U. Guth, J. Zosel, Ionics 10 (2004) 366–377.